Volume 1 | Number 1 | Jan 2013 | Pages 1–100

ChemComm

Chemical Communications
www.rsc.org/chemcomm

ROYAL SOCIETY OF CHEMISTRY

This is an *Accepted Manuscript*, which has been through the Royal Society of Chemistry peer review process and has been accepted for publication.

Accepted Manuscripts are published online shortly after acceptance, before technical editing, formatting and proof reading. Using this free service, authors can make their results available to the community, in citable form, before we publish the edited article. We will replace this *Accepted Manuscript* with the edited and formatted *Advance Article* as soon as it is available.

You can find more information about *Accepted Manuscripts* in the **Information for Authors**.

Please note that technical editing may introduce minor changes to the text and/or graphics, which may alter content. The journal's standard **Terms & Conditions** and the **Ethical guidelines** still apply. In no event shall the Royal Society of Chemistry be held responsible for any errors or omissions in this *Accepted Manuscript* or any consequences arising from the use of any information it contains.

Journal Name

COMMUNICATION

A Rechargeable Aluminum-ion Battery Utilizing a Copper Hexacyanoferrate Cathode in an Organic Electrolyte

L. D. Reed, S. N. Ortiz, M. Xiong, and E. J. Menke

Reversible aluminum intercalation / deintercalation from an organic electrolyte into copper hexacyanoferrate is presented. Evidence suggest that an aluminum-solute complex is the intercalating species. The system shows initial discharge capacities as high as 60mAh/g and reversible capacities between 5 and 14mAh/g, with capacity typically fading after 10 to 15 cycles.

To date, rechargeable batteries have primarily depended upon the well-explored electrochemistry of monovalent lithium ions. It is unquestionable that the monovalent systems have enabled technological revolutions over the last several decades and substantial improvements in power and energy density may still be possible.[1, 2] In spite of this, the potential for increased power, safety, sustainability and reduced cost as well as the promise of new insight into the fundamental nature of multivalent electrochemistry provide excellent motivation for investigation of multivalent systems. However, despite several decades of research into multivalent battery chemistries very few examples of metal-anode secondary systems based on divalent or trivalent metals exist.[3-6]

Research into multivalent chemistries for battery applications has been hindered by the difficulties in identifying suitable electrolytes and cathode materials. Most electrolytes identified to date have been highly flammable, corrosive or exhibit limited anodic stability.[7, 8] Additionally, the insertion kinetics of multivalent ions are greatly hindered by strong columbic interaction with the host lattice.[8, 9] This kinetic limitation places restrictions upon the possible cathode materials; requiring a combination of a highly open lattice to allow facile intercalation/deintercalation, sufficient redox centers near host sites to maintain charge neutrality in the presence of multivalent ions and stability against phase transitions under cycling.[3] These limitations drastically reduce the number of potential cathode materials, with Chevrel phase M_6S_8 (M = Mo, Te, Se) and analogues of Prussian blue ($Fe_4[Fe(CN)_6]_3$) being the most prominent systems showing clear evidence of electrochemical reversibility in the presence of multivalent ions.[3, 9-11]

Prussian blue, a cyano-bridged coordination polymer, has been known for hundreds of years as a pigment. Neff first reported on the electrochemical properties of Prussian blue in the late 1970's, with further work by Itaya in the 1980's.[12, 13] However, little work was done on its application as a battery material until a resurgence in interest was spurred by work from the Cui group, where they describe its use as a fast, highly reversible and stable cathode material for aqueous rechargeable systems.[14] These initial reports, which investigated monovalent aqueous electrochemistry, were followed by reports on divalent ion insertion, most notably the work by Wang et al., which describes the electrochemistry of Prussian blue analogues in the presence various divalent ions, all of which showed reversible electrochemical behavior.[15] More recently Mizuno et al. described in detail the electrochemistry of the copper-analogue of Prussian blue (copper hexacyanoferrate, CuHCF) during cycling with aqueous Mg^{2+}.[10, 16]

Based on the natural extension of this recent work we have investigated CuHCF as a cathode material for aluminum ions in an electrolyte of aluminum trifluoromethanesulfonate (aluminum triflate) dissolved in diethylene glycol dimethyl ether (diglyme). Charge/discharge curves for the aluminum triflate in diglyme on a carbon black electrode, shown in Figure 1A, exhibits purely capacitive behavior and very low charge-storage densities, while charge/discharge curves for a CuHCF electrode in an aluminum triflate in diglyme electrolyte, shown in Figure 1B, exhibit a sloping discharge potential and large hysteresis, as well as much larger charge-storage densities. The sloping discharge potential and hysteresis is characteristic of a kinetically hindered insertion reaction,[17] which has also been observed in lithium ion systems, and has been attributed to the effects of nanoscale crystallites.[18] Cyclic voltammograms (CVs) of 5:1 molar ratio diglyme:aluminum triflate on a CuHCF working electrode, shown in blue in Figure 1C, reveals little-to-no hysteresis and three broad sets of redox peaks with very slow kinetics, while CVs of 500:1 molar ratio diglyme:aluminum triflate on a CuHCF working electrode, shown in red in Figure 1C, show only capacitive effects,

a. *University of California, Merced. 5200 N. Lake Rd, Merced Ca, 95343.*
† Email: emenke@ucmerced.edu.

indicating the CuHCF is active as a cathode material only in highly concentrated electrolytes.
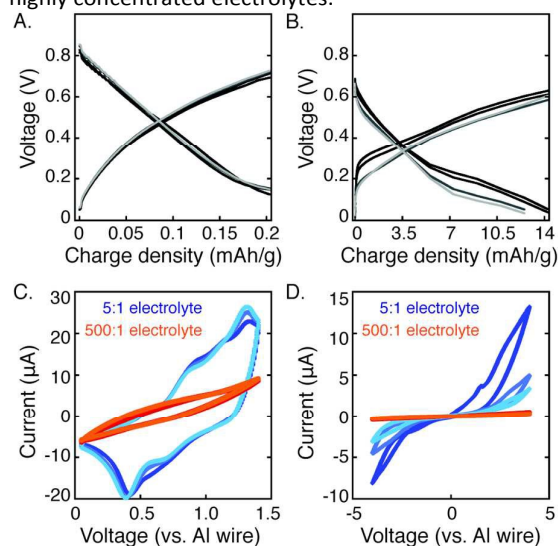

Figure 1. 2nd, 5th, 10th and 15th charge/discharge cycles (black to light grey) of A) a carbon black electrode exhibiting capacitive behavior with low charge density and B) a CuHCF electrode showing a sloping discharge curve characteristic of a single-phase discharge reaction. Cyclic voltammetry in 5:1 molar ratio diglyme:aluminum electrolyte (cycles 1-3, dark blue to light blue) and 500:1 molar ratio diglyme:aluminum electrolyte (cycles 1-3, dark red to light orange), at a 1mV/s scan rate C) of a CuHCF electrode and D) of an aluminum electrode.

While monovalent aqueous systems can access only the Fe^{2+}/Fe^{3+} couple,[14, 19] multivalent aqueous systems are able to access the redox chemistry of both Fe and Cu, as shown in recent work by Mizuno et al., due to the increased Lewis acidity and higher columbic charge density of the higher-valence ion.[10] Based on this, we hypothesize that the peaks in the CV at 0.45 volts and 0.85 volts versus Al/Al^{3+} are due the Cu^{+}/Cu^{2+} and Fe^{2+}/Fe^{3+} redox couples, respectively.[10] Furthermore, we postulate that the third peak in the cyclic voltammogram, at 1.3 volts versus Al/Al^{3+}, results from the Fe^{3+}/Fe^{4+} redox couple, as this has been shown to be accessible in other systems.[20, 21] In addition to cyclic voltammograms on the CuHCF electrode, CVs on an aluminum wire in the 5:1 and 500:1 electrolyte exhibit very different behavior. The CVs, seen in Figure 1D, clearly show that the aluminum electrode is active in the 5:1 electrolyte, although the electrode rapidly passivates, while the aluminum electrode is completely inactive in the 500:1 electrolyte. The aluminum passivation is likely due to the formation of aluminum fluoride resulting from the oxidation of aluminum in the presence of triflate, as has been reported in previous work studying the behavior of aluminum current collectors in lithium battery electrolytes.[22]

For the CuHCF cathodes, the specific capacity of the first discharge varied widely amongst tested electrodes, ranging from 10 to 60 mAh/g. In addition, the cathodes showed varying levels of capacity fade, with some cathodes failing after 10 cycles and other cathodes lasting more than 50. While the capacity fade of bi-metallic Prussian blue analogues is known to occur in lithium ion systems via phase separation,[23-

[25] the likely cause of the capacity fade here is the passivation of the aluminum anode, seen in the CV data in Figure 1D, as well as changes in the CuHCF crystallinity, discussed below.

The cycling data shown in Figure 1B portrays a reversible capacity of 14 mAh/g, based on total cathode mass, with a columbic efficiency of 89 percent for the cycles shown, which is fairly typical across samples tested. Based on a calculated theoretical capacity of 73 mAh/g for one Al^{3+} ion inserted per CuHCF unit cell versus the obtained reversible capacities of approximately 10 mAh/g, it is likely that only partial intercalation is possible when good reversible behavior is seen. Figure 2A shows the computationally optimized geometry of a diglyme-chelated aluminum ion ($Al(Di)_2^{3+}$), an extremely stable complex we expect when aluminum triflate is dissolved in diglyme, showing hexadentate coordination with the diglyme oxygens, similar to lithium-diglyme and sodium-diglyme complexes observed in solvate ionic liquids.[26, 27] Figures 2B and C show the cubic unit cell of CuHCF, with zeolitic water and vacancy sites omitted for clarity, and the powder XRD pattern obtained from the as synthesized material respectively. The reflections match the expected cubic $Cu[Fe(CN)_6]_2$ with space group Fm-3m and correlate with JCPDS 53-0084, in good agreement with prior results.[23]
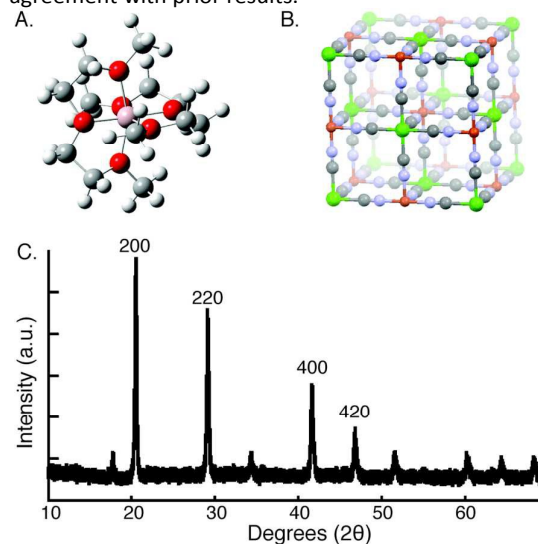

Figure 2. (A) The Gaussian optimized structure of the aluminum-diglyme complex with a diameter of approximately 7Å. (B) A representation of the cubic CuHCF unit cell, with an edge length of approximately 10Å. (C) Powder XRD of the synthesized CuHCF obtained with CoK(α) radiation of wavelength 1.79801Å.

The literature reports FeCN vacancies of approximately 25% in Prussian blue and its analogues.[28, 29] These vacancies present a larger pore diameter of approximately 5Å compared to the interstitial sites with a diameter of 3.2Å.[15] Given the calculated diameter of approximately 7Å for an $Al(Di)_2^{3+}$ complex and the high energetic barrier to desolvation of the aluminum ions it is unlikely that reversible intercalation/deintercalation would occur via routes other than the vacancy sites. Instead we hypothesize that the behavior of the CuHCF cathode in the aluminum triflate/diglyme electrolyte is governed by the aluminum/diglyme complex, rather than aluminum ions,

intercalating into FeCN vacancies in the copper-analogue Prussian blue cathode. Additionally, intercalation of the complex would minimize electrostatic interactions between the metal ion and the cathode and allow for reversible intercalation/deintercalation, similar to intercalation previously observed for magnesium intercalation into V_2O_5.[9]

Further evidence for this hypothesis can be seen in Figure 3. Figure 3A show the XRD pattern for a CuHCF electrode with a platinum current collector as prepared (black) and after soaking in the 5:1 electrolyte for 24 hours (blue), with no discernable change. However, comparing the XRD before and after the first discharge, shown in Figure 3B (black and blue, respectively), we see two changes. The first change is a shoulder appearing on the 200 peak and the second change is a decrease in the intensity of the 440, 600, and 620 peaks (at 2θ values of 60.54, 64.64, and 68.68 degrees, respectively). Additional cycling, shown in Figure 4C and 4D, further increases the broad 200 shoulder and diminishes the 440, 600, and 620 peaks. From this, we can see that the Prussian blue crystals in the electrode become smaller as we cycle the electrode, further evidence that the aluminum/diglyme complex is intercalating into the copper-analogue Prussian blue, leading to pulverization of the copper-analogue Prussian blue.
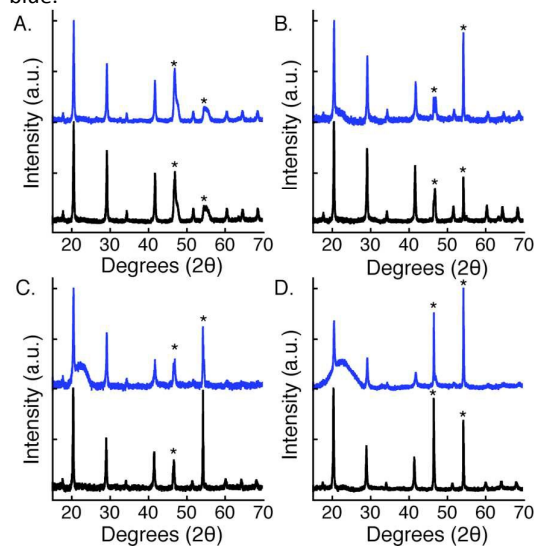

Figure 3. XRD patterns for a CuHCF/carbon black on platinum electrodes, with the platinum peaks denoted by asterisks, before (black) and after (blue) A) soaking in 5:1 electrolyte for 24 hours, B) the initial discharge, C) 15 cycles, ending on a charge cycle, and D) 17 cycles, ending on a discharge cycle.

To ascertain the effect of concentration on cycling behavior, we cycled electrodes in 5:1, 15:1, 25:1, and 50:1 molar ratio electrolytes. Comparing the cycling data for the 15:1, 25:1, and 50:1 electrolytes, shown in Figures 4A-C, respectively, with the 5:1 cycling data, shown in Figure 1B, two differences are apparent. The first difference is that decreasing the aluminum triflate concentration corresponds to an increase in the charge/discharge voltage, and a larger difference between the charge voltage and the discharge voltage. The second difference is that decreasing the aluminum triflate

concentration leads to lower, but more reproducible, capacities, and less capacity fade, as shown in Figure 4D, consistent with the hypothesis that the capacity fade is dominated by aluminum electrode passivation, which depends on the triflate concentration. This hypothesis is futher supported by the observation that after the capacity of a CuHCF electrode has dropped below 1 mAh/g, simply replacing the aluminium electrode brings the CuHCF capacity back up above 5 mAh/g, and allows for futher cycling.
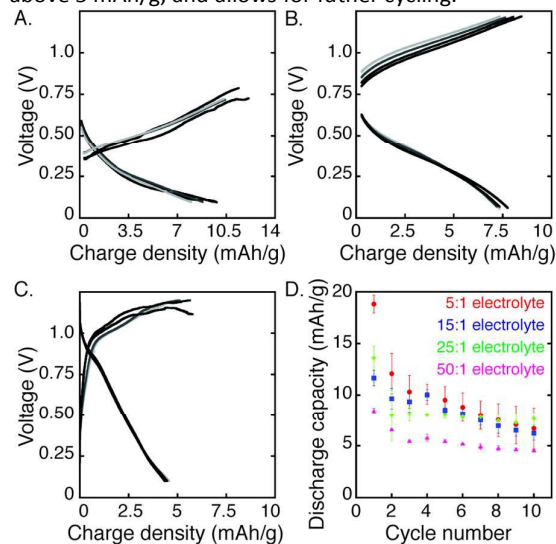

Figure 4. 2nd, 5th, 7th and 10th charge/discharge cycles (black to light grey) of a CuHCF electrode in A) 15:1 molar ratio diglyme:aluminum electrolyte, B) in 25:1 molar ratio diglyme:aluminum electrolyte, and C) in 50:1 molar ratio diglyme:aluminum electrolyte. D) Average discharge capacity for a CuHCF electrode as a function of cycle and electrolyte.

In summary, we have reported on initial electrochemical behavior for a CuHCF electrode in the presence of aluminum triflate in diglyme. This system shows the first known electrochemical cycling from an organic electrolyte containing a trivalent cation. Initial discharge capacities as high as 60mAh/g were obtained with reversible capacities between 5 and 14mAh/g, although the cell capacity typically fades after approximately 10 cycles due to some combination of material destruction in the cathode and anode passivation. Cyclic voltammograms indicate the redox activity of Fe^{2+}/Fe^{3+} and Cu^+/Cu^{2+} and also a third redox peak that may be due to the Fe^{3+}/Fe^{4+} redox couple. Capacity analysis and Gaussian calculations suggest that an aluminum/diglyme complex, rather than a free aluminum ion, is intercalating into defect sites in the CuHCF, leading to a low reversible capacity.

Notes and references

with 18 MΩ-cm water and dried under vacuum at 70°C overnight.

The composite electrode material was prepared by grinding CuHCF and carbon black together in a mortar and pestle followed by addition of pVDF in NMP to achieve a weight ratio of 80:10:10, CuHCF to carbon black to binder. For cyclic voltammetry and pre- and post-cycling XRD the resulting slurry was applied to platinum strip current collectors, which were dried under vacuum at 70°C overnight with a resultant active mass loading of approximately 2 mg/cm^2, whereas for all other cycling the resulting slurry was applied to carbon cloth current collectors, which were dried under vacuum at 70°C overnight with a resultant active mass loading of approximately 10 mg/cm^2.
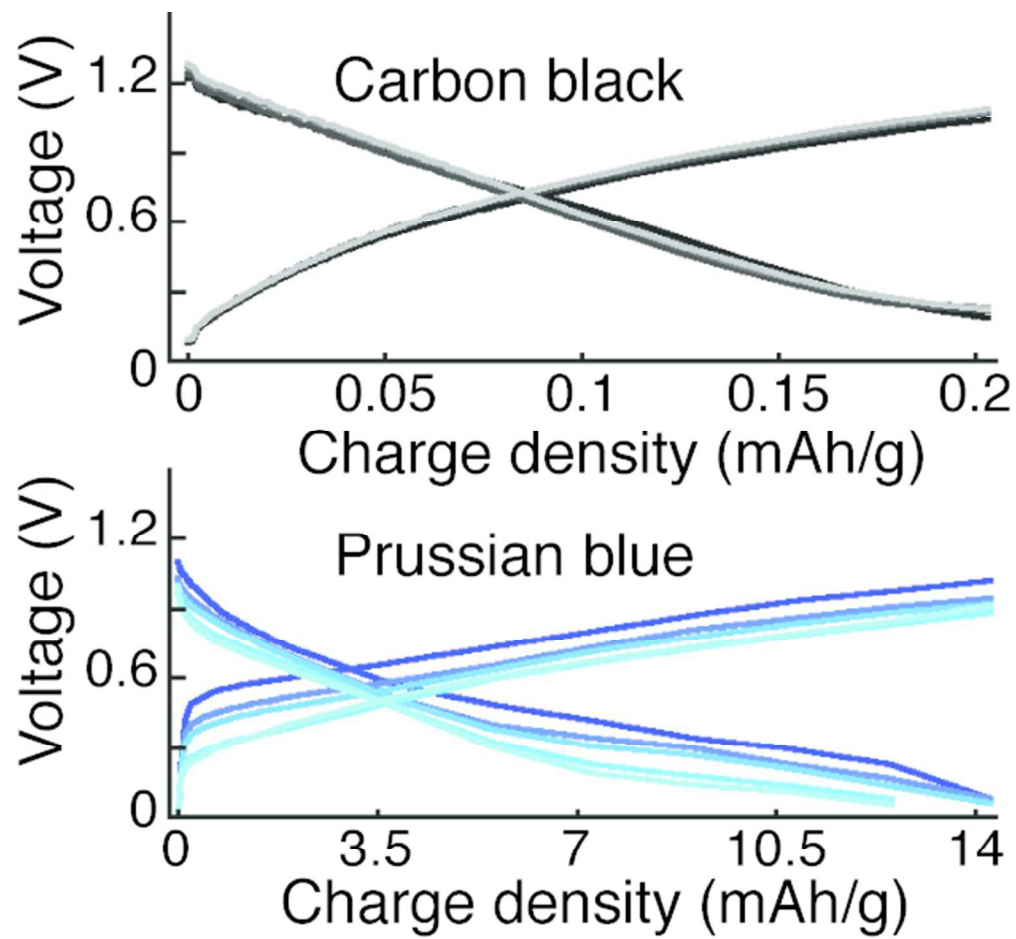
The aluminum triflate electrolytes were prepared in an argon-filled glove box (VAC Atmospheres, residual water and oxygen <0.5ppm) by addition of diglyme to the salt followed by stirring overnight.

Materials Characterization. The crystal structure of the as synthesized CuHCF was analyzed by powder X-ray diffraction on a Panalytical diffractometer from 10 to 70 degrees\. No evidence of impurities or secondary phases appears in the XRD spectrum. The electrochemical testing was carried out in a three-electrode cell using aluminum wire as the counter and reference electrodes. The cyclic voltammetry was run at a 1 mV/s scan rate, while the charge/discharge curves were collected at a C/10 rate, corresponding to a current of approximately 10 µA/cm^2 for the platinum samples and a current of approximately 50 µA/cm^2 for the carbon black samples. The data were collected on a Gamry Series G potentiostat. All charge capacity values are based on the mass of the CuHCF/carbon black/pVDF composite.

Computations. DFT calculations on the aluminum/diglyme complex were carried out in Gaussian 09 using the B3PW90 functional with a 6-311G (d) basis set.

References

1   C. K. Chan, H. L. Peng, G. Liu, K. McIlwrath, X. F. Zhang, R. A. Huggins and Y. Cui, *Nat Nanotechnol*, 2008, **3**, 31-35.

2   L. M. Suo, Y. S. Hu, H. Li, M. Armand and L. Q. Chen, *Nat Commun*, 2013, **4**.

3   D. Aurbach, Z. Lu, A. Schechter, Y. Gofer, H. Gizbar, R. Turgeman, Y. Cohen, M. Moshkovich and E. Levi, *Nature*, 2000, **407**, 724-727.

4   Y. Y. Shao, M. Gu, X. L. Li, Z. M. Nie, P. J. Zuo, G. S. Li, T. B. Liu, J. Xiao, Y. W. Cheng, C. M. Wang, J. G. Zhang and J. Liu, *Nano Lett*, 2014, **14**, 255-260.

5   R. Zhang, F. Mizuno and C. Ling, *Chemical Communications*, 2015, **51**, 1108-1111.

6   M.-C. Lin, M. Gong, B. Lu, Y. Wu, D.-Y. Wang, M. Guan, M. Angell, C. Chen, J. Yang, B.-J. Hwang and H. Dai, *Nature*, 2015, **520**, 324-328.

7   J. Muldoon, C. B. Bucur, A. G. Oliver, T. Sugimoto, M. Matsui, H. S. Kim, G. D. Allred, J. Zajicek and Y. Kotani, *Energ Environ Sci*, 2012, **5**, 5941-5950.

8   H. D. Yoo, I. Shterenberg, Y. Gofer, G. Gershinsky, N. Pour and D. Aurbach, *Energ Environ Sci*, 2013, **6**, 2265-2279.

9   E. Levi, Y. Gofer and D. Aurbach, *Chem Mater*, 2010, **22**, 860-868.

10   Y. Mizuno, M. Okubo, E. Hosono, T. Kudo, K. Oh-ishi, A. Okazawa, N. Kojima, R. Kurono, S. Nishimura and A. Yamada, *J Mater Chem A*, 2013, **1**, 13055-13059.

11   R. Y. Wang, C. D. Wessells, R. A. Huggins and Y. Cui, *Nano Lett*, 2013, **13**, 5748-5752.

12   K. Itaya, I. Uchida and V. D. Neff, *Accounts Chem Res*, 1986, **19**, 162-168.

13   V. D. Neff, *J Electrochem Soc*, 1978, **125**, 886-887.

14   C. D. Wessells, R. A. Huggins and Y. Cui, *Nat Commun*, 2011, **2**.

15   W. Wang, B. Jiang, W. Xiong, H. Sun, Z. Lin, L. Hu, J. Tu, J. Hou, H. Zhu and S. Jiao, *Sci. Rep.*, 2013, **3**.

16   Y. Mizuno, M. Okubo, E. Hosono, T. Kudo, H. S. Zhou and K. Oh-ishi, *J Phys Chem C*, 2013, **117**, 10877-10882.

17   R. A. Huggins, *Advanced Batteries*, Springer, 2009.

18   M. Okubo, Y. Mizuno, H. Yamada, J. Kim, E. Hosono, H. S. Zhou, T. Kudo and I. Honma, *Acs Nano*, 2010, **4**, 741-752.

19   C. D. Wessells, S. V. Peddada, R. A. Huggins and Y. Cui, *Nano Lett*, 2011, **11**, 5421-5425.

20   N. Yabuuchi, M. Kajiyama, J. Iwatate, H. Nishikawa, S. Hitomi, R. Okuyama, R. Usui, Y. Yamada and S. Komaba, *Nat Mater*, 2012, **11**, 512-517.

21   H. Zhou, S. Upreti, N. A. Chernova, G. Hautier, G. Ceder and M. S. Whittingham, *Chem Mater*, 2011, **23**, 293-300.

22   M. Morita, T. Shibata, N. Yoshimoto and M. Ishikawa, *Electrochim Acta*, 2002, **47**, 2787-2793.

23   D. Asakura, C. H. Li, Y. Mizuno, M. Okubo, H. S. Zhou and D. R. Talham, *J Am Chem Soc*, 2013, **135**, 2793-2799.

24   S. Kajiyama, Y. Mizuno, M. Okubo, R. Kurono, S. Nishimura and A. Yamada, *Inorg Chem*, 2014, **53**, 3141-3147.

25   M. Okubo, D. Asakura, Y. Mizuno, T. Kudo, H. Zhou, A. Okazawa, N. Kojima, K. Ikedo, T. Mizokawa and I. Honma, *Angew Chem Int Edit*, 2011, **50**, 6269-6273.

26   K. Yoshida, M. Nakamura, Y. Kazue, N. Tachikawa, S. Tsuzuki, S. Seki, K. Dokko and M. Watanabe, *J Am Chem Soc*, 2011, **133**, 13121-13129.

27   C. Zhang, K. Ueno, A. Yamazaki, K. Yoshida, H. Moon, T. Mandai, Y. Umebayashi, K. Dokko and M. Watanabe, *The Journal of Physical Chemistry B*, 2014, **118**, 5144-5153.

28   M. V. Bennett, L. G. Beauvais, M. P. Shores and J. R. Long, *J Am Chem Soc*, 2001, **123**, 8022-8032.

29   H. J. Buser, D. Schwarzenbach, W. Petter and A. Ludi, *Inorg Chem*, 1977, **16**, 2704-2710.

ChemComm Accepted Manuscript

53x50mm (300 x 300 DPI)